Journal of ELECTRICAL ENGINEERING, VOL. 61, NO. 6, 2010, 357–364

MATHEMATICAL MODELLING AND PARAMETER DETERMINATION OF RELUCTANCE SYNCHRONOUS MOTOR WITH SQUIRREL CAGE

Peter Hudák * — **Valéria Hrabovcová** **

The paper provides an analysis of reluctance synchronous motor (RSM) with asymmetrical rotor cage. Its performances during its starting up is investigated. A mathematical model is created on the basis of detailed investigation of model parameters. The RSM starting up by switching it directly across the line was simulated and verified by measurements.

K e y w o r d s: leakage inductance, magnetizing inductance, reluctance synchronous motor, reluctance torque, mathematical model

1 INTRODUCTION

The reluctance synchronous motor (RSM) is a machine working on the basis of development of reluctance torque development. The rotor configuration with the salient poles is made from the rotor of asynchronous motor if some rotor teeth are symmetrically removed (mill out). A different air gap in d and q axis enables development of a reluctance torque. The rotor cage is asymmetrical because some bars are located in the slots surrounded by iron and the other are surrounded by air, as it is shown in Fig. 1. This cage allows starting the motor directly from the grid, like the induction motors. In synchronous operation the cage acts as a damper of the oscillations in the speed. The cage parameters are important for the determination of the starting and running stability characteristics of the machine. Therefore in the past, several authors have focused on an analysis of the transient/starting performance of the RSM [1]-[5]. Mathur, [1] has created detailed mathematical model for the RSM with segmental rotor and winding on the rotor. He has derived an analytical expressions for the inductances calculation and made simulation of RSM. The coincidence between results from simulation and measurement was good but the analytical expressions were derived only for one type of rotor construction, what was unpractical.

Lawrenson [2] and Honsiger [3] focused on impact of working conditions on the transient performances of the RSM with winding on the rotor. They made a lot of the simulation and on the basis of results have created also basic recommendations for the RSM designers.

In recent years, authors [6], [7] have used the finite element method for a detailed analysis of the transient performance of the RSM. The FEM brought a lot of the advantages in the analysis but it is a time consuming method, and good FEM software is also expensive.

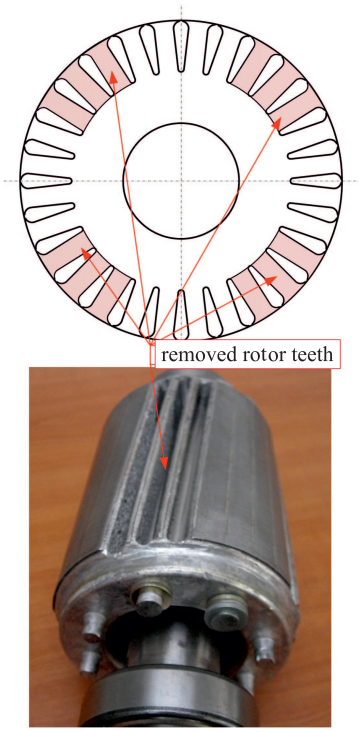

Fig. 1. Asynchronous rotor with symmetrically removed rotor teeth

In this paper, a mathematical model is created comprising very complete system of equations with demanding mathematical apparatus describing mutual linking between rotor parameters in d and q axis as well as between the stator and, the rotor. The self and mutual inductance are calculated by free FEMM [9] software.

2 MATHEMATICAL MODEL OF THE RSM WITH ASYMMETRICAL ROTOR CAGE

As it is seen in Fig. 1, the bars of the cage are distributed asymmetrically, but from the point of view of its electrical parameters, they differ in d and q axis. In

Power-one s.r.o, Areál ZTS 924, 018 41 Dubnica nad Váhom, Slovakia, peter.hudak@power-one.com; ** Faculty of Electrical Engineering, University of Žilina, Veľký Diel, 010 26 Žilina, Slovakia, valeria.hrabovcova@fel.uniza.sk

DOI: 10.2478/v10187-010-0055-y, ISSN 1335-3632

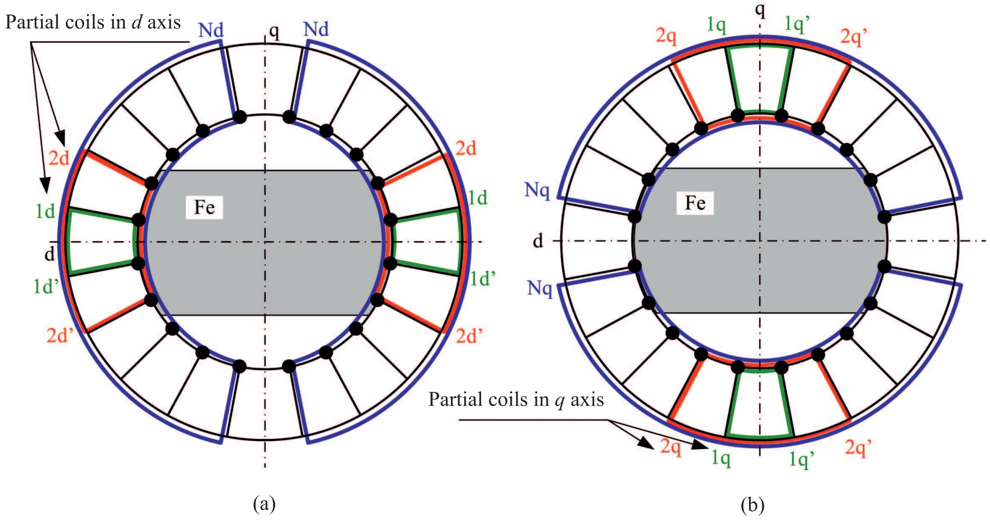

Fig. 2. Fictitious coils and loops in: (a) — d and (b) – q axis

Fig. 2, there is an illustrative view on the cross-section area of such cage with its fictitious coils and loops in d and q axis, which are numbered from 1d, 2d,... *etc*, to Nd in d axis, and from 1q, 2q,... *etc* to Nq in q axis. One coil-loop is created by 1d-1d', 2d-2d',... *etc* in d axis, the same approach is used in q axis.

For such arranged cage is created a mathematical model, which enables a detailed analysis how the cage asymmetry influences the running up and synchronizing of the RSM. The RSM mathematical model with asymmetrical cage is presented in the form, as follows

$$
\begin{aligned}
u_d &= i_d R_S + \frac{d\psi_d}{dt} - \omega_R \psi_q \\
u_d &= i_q R_S + \frac{d\psi_q}{dt} + \omega_R \psi_d \\
u_0 &= i_0 R_S + \frac{d\psi_0}{dt} \\
0 &= i'_{1d} R'_{11d} + \frac{d\psi'_{1d}}{dt} \\
&\dots \\
0 &= i'_{Nd} R'_{NdNd} + \frac{d\psi'_{Nd}}{dt} \\
0 &= i'_{1q} R'_{11q} + \frac{d\psi'_{1q}}{dt} \\
&\dots \\
0 &= i'_{Nq} R'_{NqNq} + \frac{d\psi'_{Nq}}{dt}
\end{aligned}
\tag{1a}
$$

where

$$
R'_{11d} = \frac{3}{2}\frac{N_{wS1}^2}{N_{w1d1}^2} R_{11d} \tag{1b}
$$

is the rotor resistance R_{11d} (resistance of the fictitious coil 1d-1d') referred to the stator. In the same way also the other rotor resistances are referred to the stator.

and

$$
\begin{aligned}
\psi_d &= (L_{\sigma S} + L_{\mu d}) i_d + L_{\mu d}(i'_{1d} + i'_{2d} + \dots + i'_{Nd}) \\
\psi_q &= (L_{\sigma S} + L_{\mu q}) i_q + L_{\mu q}(i'_{1q} + i'_{2q} + \dots + i'_{Nq}) \\
\psi_0 &= L_{\sigma S} i_0 \\
\psi'_{1d} &= (L'_{\sigma 1d} + L_{\mu d}) i'_{1d} + L_{\mu d}(i_d + i'_{2d} + \dots + i'_{Nd}) \\
\psi'_{1q} &= (L'_{\sigma 1q} + L_{\mu q}) i'_{1q} + L_{\mu q}(i_q + i'_{2q} + \dots + i'_{Nq}) \\
\psi'_{2d} &= (L'_{\sigma 2d} + L_{\mu d}) i'_{2d} + L_{\mu d}(i_d + i'_{1d} + i'_{3d} + \dots + i'_{Nd}) \\
\psi'_{2q} &= (L'_{\sigma 2q} + L_{\mu q}) i'_{2q} + L_{\mu q}(i_q + i'_{1q} + i'_{3q} + \dots + i'_{Nq}) \\
&\dots\dots \\
\psi'_{Nd} &= (L'_{\sigma Nd} + L_{\mu d}) i'_{Nd} + L_{\mu d}(i_d + i'_{1d} + \dots + i'_{(N-1)d}) \\
\psi'_{Nq} &= (L'_{\sigma Nq} + L_{\mu q}) i'_{Nq} + L_{\mu q}(i_q + i'_{1q} + \dots + i'_{(N-1)q})
\end{aligned}
\tag{2a}
$$

where for example ψ'_{Nd} – is a linkage flux of the rotor coil Nd referred to the stator,

$$
L'_{\sigma Nd} = \frac{3}{2}\frac{N_{wS1}^2}{N_{wNd1}^2} L_{\sigma Nd}
$$

is a rotor leakage inductance $L_{\sigma Nd}$ referred to the stator, on the basis of the so called "winding functions", where

$$
\frac{N_{wS1}}{N_{wNd1}} = \frac{2}{3}\frac{L_{\mu d}}{L_{dNd}} \Rightarrow \frac{3}{2}\frac{N_{wS1}^2}{N_{wNd1}^2} = \frac{2}{3}\left(\frac{L_{\mu d}}{L_{dNd}}\right)^2 \tag{2b}
$$

N_{wSl} – is a fundamental component of the winding function of the stator and N_{wNdl} – is a fundamental component of the winding function of the rotor coil Nd.

The voltage equations are completed by the equation of electromagnetic torque which is derived from the air-gap power p_δ

$$
\begin{aligned}
p_\delta &= \left(\frac{3}{2}\right)\omega_R(\psi_d i_q - \psi_q i_d) = \left(\frac{3}{2}\right) p\Omega(\psi_d i_q - \psi_q i_d) \\
&\Rightarrow m_e = \left(\frac{3}{2}\right) p(\psi_d i_q - \psi_q i_d)
\end{aligned}
\tag{3}
$$

and the equation for mechanical angular speed Ω

$$\frac{\mathrm{d}\Omega}{\mathrm{d}t} = \frac{1}{J}(m_e - m_L)$$

where p – is the number of pole pairs, J – is moment of inertia, and m_L – is the load torque.

To solve this system of equation, not only voltages applied to the RSM terminals but also the resistances and inductances of the investigated RSM are needed to know.

The rating and parameters of the asynchronous motor, the rotor which has been rearranged to create the salient poles are as follows: 3 phase, 4 pole ASM 4AP90L, 1500 W, 400/380 V, 3.4/3.6 A, 1410 rpm, $\eta = 77\%, \cos\phi = 0.82$, resistance of stator winding at 20 °C is $R_{S20} = 5.422\,\Omega$, and at 75 °C is $R_{S75} = 6.575\,\Omega$, the resistance of the rotor bar is $R_{bar20} = 91.33\,\mu\Omega$, $R_{bar75} = 117.55\,\mu\Omega$, the part of the ring belonging to one bar (or between two adjacent bars) $R_{ring20} = 1.641\,\mu\Omega$, $R_{ring75} = 2.05\,\mu\Omega$.

3 CALCULATION OF SELF AND MUTUAL INDUCTANCES

To get the self and mutual inductances of the windings, the FEM analysis has been used. The self inductances are calculated by means of expression

$$L_{jj}(\theta_R) = \frac{\psi_j(\theta_R)}{i_j} \tag{4a}$$

where

$$\psi_j(\theta_R) = l_{FeS}\frac{z_Q}{n_{pp}}\sum_{i=1}^{Q_S} k_{ji}\frac{1}{S_{di}}\int_{S_{di}} A dS_d \tag{4b}$$

and z_Q – is the number of conductor in a slot, n_{pp} – is the number of parallel conductor in a slot, Q_S – is the number of stator slots, k_{ji} – is a factor saying how the winding in i-slot is oriented.

The mutual inductances are calculated by means of similar expression

$$L_{jk}(\theta_R) = \frac{\psi_k(\theta_R)}{i_j} \tag{5}$$

where $\psi_k(\theta_R)$ – is the leakage flux of k-coil, which will be calculated by means of (4b).

In the shown way the waveforms of self and mutual stator inductances as a function of rotor position have been calculated. The Fourier series of these waveforms have shown that most dominant are zero and second space harmonic components. The other ones can be neglected. Therefore more convenient the inductances can be expressed as follows

$$\begin{aligned}
L_{aa} &= L_{\sigma S} + L_0 + L_2\cos(2\theta_R)\\
L_{bb} &= L_{\sigma S} + L_0 + L_2\cos(2\theta_R - 2\pi/3)\\
L_{cc} &= L_{\sigma S} + L_0 + L_2\cos(2\theta_R + 2\pi/3)\\
L_{ab} &= L_{ba} = -M_0 + M_2\cos(2\theta_R + 2\pi/3)\\
L_{bc} &= L_{cb} = -M_0 + M_2\cos(2\theta_R)\\
L_{ac} &= L_{ca} = -M_0 + M_2\cos(2\theta_R - 2\pi/3)
\end{aligned} \tag{6}$$

If these expressions are introduced to the expressions of linkage flux, *eg* Ψ_d, the further deriving results in expression for synchronous inductance in d and q axis, respectively

$$\begin{aligned}
L_d &= \frac{2}{3}\left(L_{\sigma S} + L_0 + \frac{L_2}{2} + M_0 + M_2\right)\\
L_q &= \frac{2}{3}\left(L_{\sigma S} + L_0 - \frac{L_2}{2} + M_0 - M_2\right)
\end{aligned} \tag{7}$$

where: $L_{\sigma S}$ – is stator leakage inductance, consisting of leakage inductance of end winding $L_{\sigma endS}$ and differential leakage inductance $L_{\sigma difd}$

The values of synchronous inductance for here investigated RSM for current $I_S = I_{0\_nom} = 3.2$ A are as follows

$$L_d = \frac{2}{3}(L_{\sigma endS} + L_{\sigma difd} + L_0 + \frac{L_2}{2} + M_0 + M_2) =$$
$$= \frac{2}{3}(4.78 + 10.6 + 152.8 + \frac{31.82}{2} + 62.3 + 86.54) \times 10^{-3}$$

giving: $L_d = 222.02$ mH

$$L_q = \frac{2}{3}(L_{\sigma endS} + L_{\sigma difq} + L_0 - \frac{L_2}{2} + M_0 - M_2) =$$
$$= \frac{2}{3}(4.78 + 31.3 + 152.8 - \frac{31.82}{2} + 62.3 - 86.54) \times 10^{-3}$$

giving: $L_q = 99.22$ mH

These values are compared with measured in no-load test, load test, DC delay test and are given in Tab. 1.

Table 1. Comparison of synchronous inductances gained by various methods

		L_d (mH)	X_d (Ω)	L_q (mH)	X_q (Ω)
test,	no-load	225.4	70.8		
meas-	load			89.54	28.13
ured	DC delay	232.9	73.20	124.1	39.0
calculated by (7)		222.02	69.75	99.22	31.17
diferences between measurement and calculation in %		-1.50 *vs* #1		10.80 *vs* #2	
		-4.67 *vs* #3		-20.00 *vs* #3	

Table 2. Factors needed to refer parameters of rotor partial coils to the stator windings

partial coil	1d	2d	3d	4d
$L_{\mu d}$ (mH)		417.346		
L_{dNd} (mH)	0.55×10^{-3}	1.872	3.42	3.44
$L_{\mu d}/L_{dNd}$	7.47×10^{5}	222.94	121.92	121.18
f_d	3.72×10^{11}	33135.1	9910.31	9798.8

calculated at $I_s = 0.5$ A, $f_d = \frac{2}{3}(L_{\mu d}/L_{dNd})^2$

partial coil	1q	2q	3q	4q
$L_{\mu q}$ (mH)		135.074		
L_{qNq} (mH)	2.44×10^{-2}	6.68×10^{-2}	1.379	1.82
$L_{\mu q}/L_{qNq}$	5.54×10^{3}	2.02×10^{3}	97.95	74.21
f_q	2.04×10^{7}	2.72×10^{6}	6396	3672

calculated at $I_s = 0.5$ A, $f_q = \frac{2}{3}(L_{\mu d}/L_{dNd})^2$

The mutual inductances between stator and partial rotor coils as a function of rotor position, have been calculated on the basis of equation (5) and FEM. The Fourier series has been shown, that dominant harmonic components are fundamental and third one, therefore the inductances can be expressed as follows

$$\begin{aligned}
L_{aNd} &= L_{\max aNd_1}\cos(\theta_R) + L_{\max aNd_3}\cos(3\theta_R)\\
L_{bNd} &= L_{\max bNd_1}\cos(\theta_R - 2\pi/3) + L_{\max bNd_3}\cos(3\theta_R)\\
L_{cNd} &= L_{\max cNd_1}\cos(\theta_R + 2\pi/3) + L_{\max cNd_3}\cos(3\theta_R)\\
L_{aNq} &= L_{\max aNq_1}\sin(\theta_R) + L_{\max aNq_3}\sin(3\theta_R)\\
L_{bNq} &= L_{\max bNq_1}\sin(\theta_R - 2\pi/3) + L_{\max bNq_3}\sin(3\theta_R)\\
L_{cNq} &= L_{\max cNq_1}\sin(\theta_R + 2\pi/3) + L_{\max cNq_3}\sin(3\theta_R)
\end{aligned} \tag{8}$$

In these expressions are introduced to linkage flux Ψ_{1d}, the next rearranging will result in the final expression for mutual inductance $L_{d1d} = L_{maxa1d1} = L_{maxb1d1} = L_{maxc1d1}$. The same approach will be introduced for L_{q1q}. The factors needed to refer parameters of rotor partial coils to the stator windings are in Tab.2, where L_μ – is the magnetizing inductance investigated like a difference between synchronous inductance, calculated according (7) for stator current $I_S = 0.5$ A, and leakage inductance of the stator.

4 CALCULATION OF ROTOR RESISTANCES

The resistances of partial rotor coils will consist of the bar resistance and belonging part of the ring. For a partial coil Nd in d -axis it will be calculated as follows (similar for Nq in q -axis)

$$R_{Nd} = 2p\,(N_{bar}R_{bar} + N_{ring}R_{ring}) \tag{9}$$

where: N_{bar} – is number of bars of given partial coil belonging to one pole, N_{ring} – is number of ring parts connected bars of partial coil belonging to one pole.

The calculated values of resistances for investigated motor are as follows: $R_{bar20} = 91.33\ \mu\Omega$; $R_{bar75} = 117.55\ \mu\Omega$; $R_{ring20} = 1.641\ \mu\Omega$; $R_{ring75} = 2.051\ \mu\Omega$. The real values of rotor resistances as well as those referred to the stator side in Tab. 3

Table 3. Resistances of the partial coils

partial coil	1d	2d	3d	4d
R_{bar75} ($\mu\Omega$)	250.16*	125.08	117.55	117.55
N_{ring}	0	4	8	12
R_{Nd} ($\mu\Omega$)	2001.28	1033.4	1006.03	1038.8
referred value R'_{Nd} ($\mu\Omega$)	7.46×10^{8}	34.24	9.97	10.17

$N_{bar} = 2$, $R_{ring75} = 2.051\ \mu\Omega$

partial coil	1q	2q	3q	4q
R_{bar75} ($\mu\Omega$)	117.55	117.55	125.08*	250.16
N_{ring}	2	6	10	14
R_{Nq} ($\mu\Omega$)	956.8	989.6	1082.68	2116.1
referred value R'_{Nq} ($\mu\Omega$)	19585.7	2693.7	6.925	7.77

5 CALCULATION OF LEAKAGE INDUCTANCES

The leakage inductances of partial rotor coils consist of leakage inductance of slot, end connectors and differential leakage inductance. In d -axis (similar in q -axis) for Nd coil it will be

$$L_{\sigma Nd} = L_{\sigma dR} + L_{\sigma ringR} + L_{\sigma difR} \tag{10}$$

All three components of (10) will be analyzed in more details below.

5.1. Slot leakage inductance

The well known expression for slot leakage inductance will be applied for the investigated RSM

$$L_{\sigma dR} = 2pq\left(\frac{N_R}{pq}\right)^2 \Lambda_{dR} \tag{11}$$

where $2pq$ – is the total number of slots for given winding. For here investigated RSM it is 8 slots, 2 slots per pole (see Fig. 1), $\frac{N_R}{pq}$ – is the number of conductor in the given slot, here it is 1, because in each slot there is one bar, Λ_{dR} – is the slot magnetic conductivity. Only this parameter

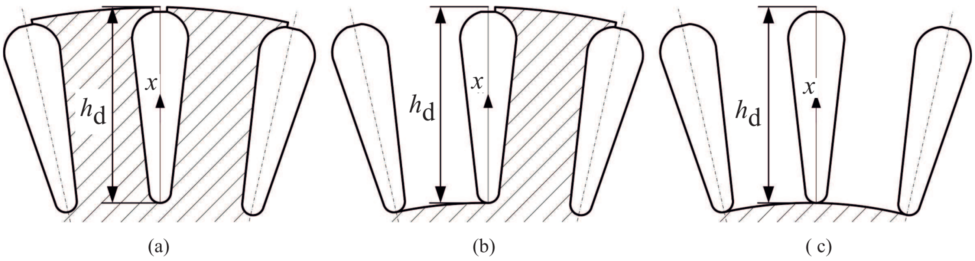

Fig. 3. Three basic positions of the rotor slot (bar) with regard to its surrounding: (a) – the whole bar is surrounded by iron, (b) – half of the bar is surrounded by iron and a half by the air, (c) – the whole bar is in the air

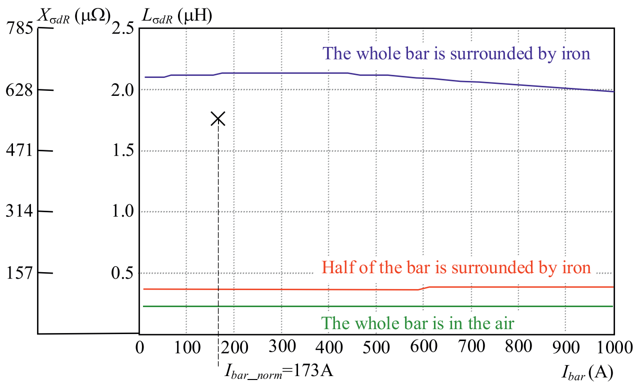

Fig. 4. Slot leakage inductance versus slot current. The cross means value calculated by means of expression valid for slot of squirrel cage

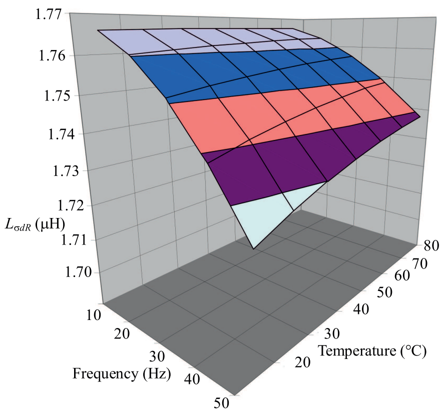

Fig. 5. Slot leakage inductance versus temperature and frequency

is unknown and will be investigated by means of FEM. This method has been evaluated for IM in [8], here will be accommodated for the salient pole of the RSM. Here the rotor bar in the slot can appear in these typical positions according the surrounding of the slot, see Fig. 3.

The procedure of the slot leakage inductance FEM calculation can be described in the following steps

1 – the rotor bar is fed by a current, at which the inductance will be calculated,

2 – the magnetic flux density along the slot axis (see Fig. 3) is gained by means of FEM,

3 – the leakage slot flux is gained as an integral of the flux density along the height of the slot (see Fig. 3 : the arrow shows a direction of integration):

$$\psi_{\sigma d} = l_{Fe} \int_0^{h_d} B_{\sigma d} dx \tag{12}$$

4 – then the magnetic conductivity can be calculated

$$\Lambda_d = \frac{\psi_{\sigma d}}{z_{qR} I_{\max d}} \tag{13}$$

where, z_{qR} – is the number of conductors in the investigated slot, here it is 1, I_{maxd} – is the maximum of the current flowing in the investigated winding (here in the bar).

Table 4. Distribution of the current in the partial rotor coils in d- and q-axis and corresponding slot leakage inductance

	d – axis rotor current (A)			
	I_{1d}	I_{2d}	I_{3d}	I_{4d}
	0	72.9	154	164
$L_{\sigma dR}$ (μH)	1*	2.15	0.48	0.08
$X_{\sigma dR}$ ($\mu\Omega$)	314*	675.4	131.3	25.13

$I_S = 3.4$ A, $B_{\delta 1} = 0.925$ T

	q – axis rotor current (A)			
	I_{1q}	I_{2q}	I_{3q}	I_{4q}
	38.5	68	170	241
$L_{\sigma qR}$ (μH)	0.046	0.05	2.165	1.06*
$X_{\sigma qR}$ ($\mu\Omega$)	14.45	15.71	680.1	333*

$I_S = 3.4$ A, $B_{\delta 1} = 0.425$ T

* these partial coils have only half number of the rotor bars in comparison with other partial coils therefore their slot leakage inductance is 1/2 lower, see also (11).

Table 5. Leakage inductances and reactances of the cage ring

partial		d – axis		
coil	1d	2d	3d	4d
n_{ring}	0	4	8	8
$L_{\sigma ring}$ (μH)	0	0.46	0.92	0.92
$X_{\sigma ring}$ ($\mu\Omega$)	0	144.67	289.30	289.30

partial		q – axis		
coil	1q	2q	3q	4q
n_{ring}	0	0	4	8
$L_{\sigma ring}$ (μH)	0	0	0.46	0.92
$X_{\sigma ring}$ ($\mu\Omega$)	0	0	144.67	289.30

Table 6. Differential leakage inductance for rotor partial coils in d- and q- axis

partial		d – axis		
coil	1d	2d	3d	4d
I_R (A)	0	72.9	154	164
$L_{\sigma difR}$ (μH)	0	8.14	4.22	3.92
$X_{\sigma difR}$ (mΩ)	0	2.56	1.33	1.23

partial		q – axis		
coil	1q	2q	3q	4q
I_R (A)	38.5	68	170	214
$L_{\sigma difR}$ (μH)	0.15	0.19	8.19	15.01
$X_{\sigma difR}$ (mΩ)	0.045	0.062	2.57	4.72

Once the magnetic conductivity is known, the slot leakage inductance can be calculated on the basis of (11). In Fig. 4 there are its values as a function of current for all three typical slot positions according the Fig. 3.

The slot leakage inductance (reactance) for bars surrounded from both sides by iron are influenced also by skineffect. Unsaturated slot leakage inductance as a function of temperature and frequency is in Fig. 5. Skineffect is negligible in the bars surrounded by air from one or from both sides (see Fig. 5).

The calculated slot leakage inductances will be used in the next chapter in simulation of the RSM running-up. The current of each partial rotor coil is different, what is seen in Tab. 4.

5.2 End connectors leakage inductance of the rotor asymmetrical cage

The leakage inductance (reactance) of the cage end connectors is calculated for the part of the ring lying between the two adjacent bars. Because of rotor salient poles, there are two possible positions of the investigated parts of the ring: at first, in d -axis, the ring touches the iron of the teeth and second, the ring is surrounded by air in q -axis. The first case is identical with the ring of induction machine and can be calculated by the same procedure and expressions. For example for the partial rotor coil 2d, L_σ will be calculated as follows $L_{\sigma ring_2d} = 2pn_{ring}L_{\sigma ring} = 2 \times 2 \times 4 \times 28.7806 \times 10^{-9} = 0.4605\,\mu$H, where: n_{ring} – is the number of the ring parts belonging to investigated partial coil, touching iron teeth on one pole.

If the ring is surrounded by air, the leakage reactance is so small that can be neglected. In Tab. 5 there are calculated values of leakage inductances and reactances of the partial rotor coils.

5.2 Differential leakage inductance

A differential leakage inductance means an influence of space harmonics to the winding by which it was created. These harmonics induce in the winding voltage harmonics, which increase winding reactance. The investigated RSM has salient poles on the rotor with different air-gap in d- and q- axis, therefore the method obviously used for induction machine can not be employed.

The calculation for the rotor partial coils will be in the following steps:

1 – by means of FEM the rotor partial coils is fed by the same current as it was done for leakage inductance (see Tab. 4) to be able to get a waveform of flux density along the air-gap

2 – a Fourier series is done for the flux density waveform

3 – for each space harmonic of the flux density $B_{\delta vR}$ the magnetic flux is calculated

$$\phi_{\nu R} = \frac{2}{\pi}\frac{\tau_{pR}}{\nu} l_{FeR} B_{\delta\nu R} \tag{14}$$

where, $\tau_p = \frac{\pi d_R}{2p}$ -- is the pole pitch of the rotor, l_{FeR} – is a length of rotor iron stack, $B_{\delta vR}$ – is the magnitude of ν-th harmonic magnetic flux density, which was induced in the air-gap if the rotor partial coil was excited.

4 – the harmonics of magnetic flux calculated in the point 3 the induced voltage will be calculated

$$U_{\nu R} = \sqrt{2}\pi\phi_{\nu R} k_{wRv} f_{1R} N_R \tag{15}$$

where, N_R – is the number of turns of a partial rotor coil, in our case $N_R = 4$, because on each pole of the rotor there is one turn of partial rotor coil crated by two bars and corresponding parts ring, k_{wRv} – is the winding factor of the partial rotor coil for ν-th harmonic, in our case $k_{wRv} = 1$, f_{1R} – is the frequency of fundamental harmonic. In our case $f_{1R} = 50$Hz because we will

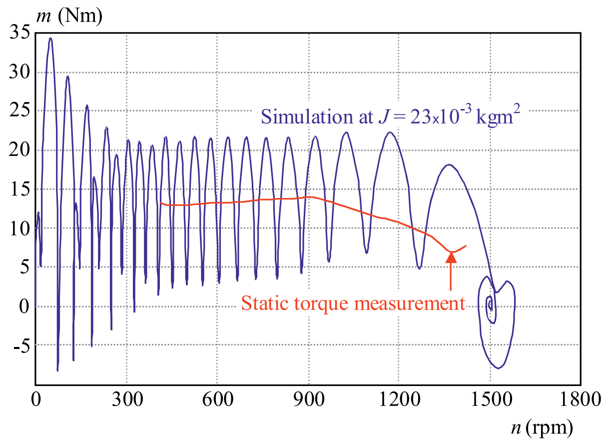

Fig. 6. Comparison of torque simulation and measurement, at the moment of inertia $J = 23 \times 10^{-3}$ kgm ^{2}

analyze the running up of the RSM, at which the rotor frequency is identical with the stator one.

5 – at the end the differential leakage inductance (reactance) will be calculated

$$X_{\sigma difR} = \frac{\sqrt{\sum U_{vR}^2}}{I_R} = \frac{\sqrt{U_{3R}^2 + U_{5R}^2 + U_{7R}^2 + \dots}}{I_R}$$
$$L_{\sigma difR} = \frac{X_{\sigma difR}}{2\pi f_{1R}} \tag{16}$$

The results gained on the basis above described procedure are seen in Tab. 6.

In Tab. 7 there are real values of all components of leakage inductances as well as their values referred to the stator. Now we have all parameters needed for simulation and we can do it.

Table 7. Leakage inductances of the rotor partial coils

partial coil	1d	2d	3d	4d
$L_{\sigma 1R}$ (μH)	1	2.15	0.418	0.08
$L_{\sigma ringR}$ (μH)	0	0.461	0.921	0.921
$L_{\sigma 1ifR}$ (μH)	0	2.14	4.224	3.917
$L_{\sigma Nd}$ (μH)	1	10.75	5.563	4.918
reffered values				
$L'_{\sigma Nd}$ (mH)	3.73×10^8	356.21	55.13	48.15
$X'_{\sigma Nd}$ (Ω)	1.17×10^8	111.91	17.32	15.13

partial coil	1q	2q	3q	4q
$L_{\sigma 1R}$ (μH)	0.046	0.05	2.17	1.06
$L_{\sigma ringR}$ (μH)	0	0	0.461	0.921
$L_{\sigma 1ifR}$ (μH)	0.145	0.197	8.19	15.1
$L_{\sigma Nd}$ (μH)	0.191	0.247	10.82	17.07
reffered values				
$L'_{\sigma Nd}$ (mH)	3909.7	672.33	69.17	62.68
$X'_{\sigma Nd}$ (Ω)	1228,3	211.22	21.72	19.69

Table 8. Comparison of the simulated and measured steady state values

parameters	simulation	measurement	difference
I_{0N} (A)	2.694	3.22	-16.3%
I_{SN} (A)	4.2	4.55	-7.7%
ϑ_L (deg)	19.42	17.5	+10.97%

measured at $m_L = 8$ Nm

6 SIMULATION OF THE RSM STARTING BY SWITCHING IT DIRECTLY ACROSS THE LINE

To be able to verify a correctness of the derived mathematical model as well as parameters of the rotor partial coils referred to the stator side, a simulation of the RSM starting by switching it directly across the line was made.

For the simulation model also magnetizing inductances in d- and q- axis are needed. They will be calculated as a difference between synchronous inductance, calculated above for the stator current $I_S = 3.2$ A, and leakage inductance of the stator (see Tab. 1)

$$\begin{aligned} L_{\mu d} &= L_d - L_{\sigma dS} - L_{\sigma ringS} - L_{\sigma difS\_d} = \\ &= 222.02 \times 10^{-3} - 4.878 \times 10^{-3} - 4.78 \times 10^{-3} \\ &\quad - 10.63 \times 10^{-3} = 201.732 \text{ mH}, \end{aligned}$$

$$\begin{aligned} L_{\mu q} &= L_q - L_{\sigma dS} - L_{\sigma ringS} - L_{\sigma difS\_q} = \\ &= 99.22 \times 10^{-3} - 4.878 \times 10^{-3} - 4.78 \times 10^{-3} \\ &\quad - 31.33 \times 10^{-3} = 58.232 \text{ mH}. \end{aligned}$$

The other parameter is moment of inertia, which will be taken the same as of the original induction motor. The simulation was made for the RSM starting by switching it directly across the line in no-load condition, and in time $t = 1$ s the rated load $m_L = 8$ Nm was applied to the RSM rotor. The simulation results have been verified by measurements. In Tab. 8 there are simulated and measured values of the important variables in the steady-state conditions. It is see that the deviation is in acceptable rate.

The derived mathematical model enables to investigate also transients. In Fig. 6 there is shown comparison of the simulation and static torque measurement. It is see that the coincidence is very good, what confirms that the mathematical model and parameters are correct.

The further measurement which has verified the simulation model was made at the reduced voltage 120 V rms to find out waveforms of the speed, torque and stator current, which are seen in Fig. 7 and Fig. 8. The measured values of the torque have been taken by the torque transducer of the HBM, type T34N.

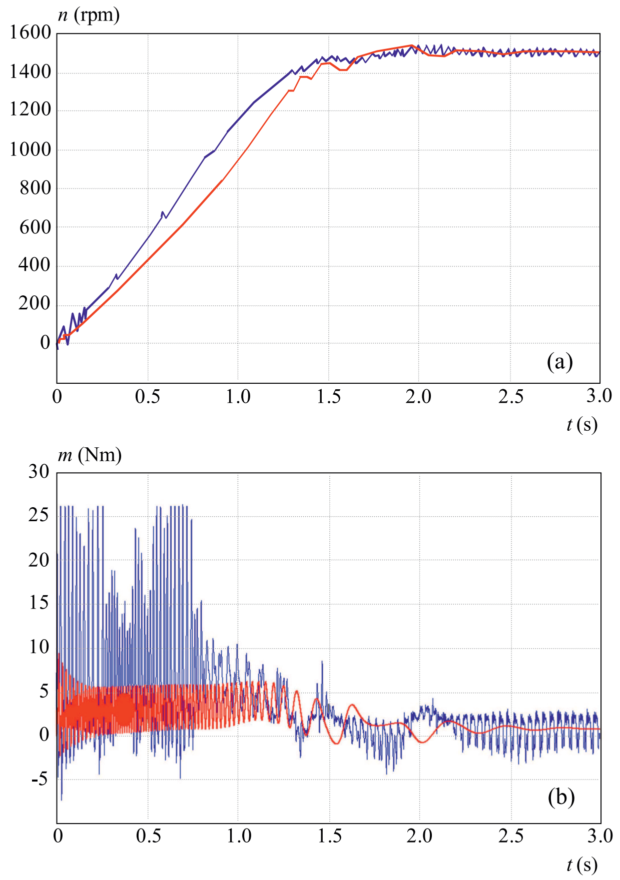

Fig. 7. Comparison the simulated and measured waveform of (a) – the speed, and (b) – the torque of the RSM at 120 V rms, $J = 23 \times 10^{-3}$ kgm ^{2}

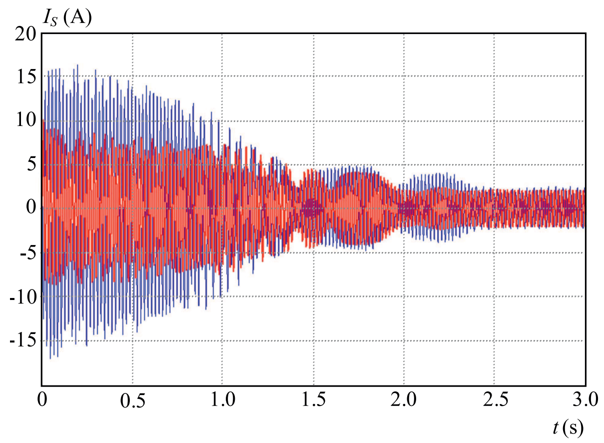

Fig. 8. Comparison the simulated and measured waveform of the stator current of the RSM at 120 V rms $J = 23 \times 10^{-3}$ kgm^2

7 CONCLUSION

A mathematical model of the RSM with asymmetrical rotor cage has been created and a detailed description of its parameters investigation is provided. The correctness of the parameters as well as of the whole model has been verified by simulations and measurements. It was shown that during the RSM starting by switching it directly across the line a coincidence of the simulated and measured waveforms of the speed, current and torque is very good. This fact confirms that the developed mathematical model is correct and can be employed for analysis of the RSM behaviour.

Acknowledgment

This work was supported by VEGA 1/0809/10 and by the Slovak Research and Development Agency under the contract No. APVT-20-39602.

References

[1] MATHUR, R. M.: The Starting Performance of Segmental-Rotor Reluctance Machines, PhD thesis, University of Leeds, October 1969.

[2] LAWRENSON, P. J.—MATHUR, R. M.—STEPHENSON, J. M.: Transient Performance of Reluctance Machines, Proceeding IEE **118** No. 6 (1971), 777–783.

[3] HONSINGER, V. B.: Steady-State performance of reluctance synchronous machines, IEEE Trans on Power apparatus and Systems **PAS90(1)** (1971), 305–317.

[4] BOLDEA, I.: Reluctance Synchronous Machine and Driverss, Clarendon/Oxford, Oxford, UK, 1996.

[5] KOVACS, K. P.—RACZ, I.: Transiente Vorgänge in Wechselstrommachinen, Verlag der Ungarischen Akademie der Wissenschaften, Budapest, 1959.

[6] NAM, H.—PARK, S. B.—KANG, G. H.—HONG, J. P.—EOM, J. B.—JUNG, T. U.: Design to improve starting performance of line-start synchronous reluctance motor for household appliances, Industry Applications Conference, 39th Annual Meeting 2004 **1** (3-7 October 2004), 78–85.

[7] J. KUDLA, J.—MIKSIEWICZ, R.: Comparison of Starting Properties of Squirrel-Cage and Synchronous Reluctance Motors, Basing on Field-Circuit Calculation, Joint Czech-Polish Conference on Project GACR Project 102/03/0813 "Low Voltage Electrical Machines", Slapanice u Brna, (November 15-16, 2004), 61–68.

[8] JANOUŠEK, J.: Identification of the IM parameters for the electric drive application, PhD thesis, University of Žilina, 2002.

[9] MEEKER, D. C.: Finite Element Method Magnetics v.4.2, Apr. 1, 2009 [Online] http://femm.foster-miller.net/wiki/HomePage.

Received 12 March 2010

Peter Hudák was born in Slovakia in 1977. He received his MSc degree in electrical engineering from the University of Zilina (SK), in 2000, and the PhD degree in 2008. He is currently a R&D engineer in the Power-one. His research activity focused on electric machines, mainly on reluctance synchronous motor, and design of the switch mode power supplies (SMPS).

Valéria Hrabovcová graduated in electrical engineering from the University of Žilina in Žilina, gained her PhD in electrical engineering from Slovak University of Technology in Bratislava in 1985. She is a professor of electric machines at the University of Žilina at undergraduate and postgraduate levels. Her professional working areas are electronically commutated electric machines.